

(Anti)proton and Pion Source Sizes and Phase Space Densities in Heavy Ion Collisions

Michael Murray

Cyclotron Institute, Texas A&M University, College Station, TX 77843-3366

June 20, 2018

Abstract

NA44 has measured mid-rapidity deuteron spectra from AA collisions at $\sqrt{s_{nn}} \approx 18$ GeV at the CERN SPS. Combining these spectra with published p , \bar{p} and \bar{d} data allows us to calculate, within a coalescence framework, p and \bar{p} source sizes and phase space densities. These results are compared to π^\pm source sizes measured by Hanbury-Brown Twiss, HBT, interferometry and phase densities produced by combining pion spectra and HBT results. We also compare to pA results and to lower energy (AGS) data. The \bar{p} source is larger than the proton source at $\sqrt{s_{nn}} = 17.3$ GeV. The phase space densities of π^+ and p are not constant but grow with system size. Both π^+ and proton radii decrease with m_T and increase with $\sqrt{s_{nn}}$. Pions and protons do not freeze-out independently. The nature of their interaction changes as $\sqrt{s_{nn}}$ and the π/p ratio increases.

Relativistic heavy ion collisions provide a mechanism to heat and compress nuclear matter to temperatures and energy densities comparable to those of the early universe when it was still a plasma of quarks and gluons. Such a state may be fleetingly restored in these collisions where temperatures of $T = 168 \pm 3$ MeV and energy densities $\epsilon = 3$ GeV/fm³ are observed [1, 2]. These values are close to those of the phase transition found in lattice calculations [3]. If such a hot and dense state were formed one would expect a large increase in entropy and possibly a saturation of the density of particles in phase space. The coalescence of nucleons into deuterons is sensitive to both their spatial and momentum correlations. In

this paper we report p , \bar{p} and π^+ source sizes measured by coalescence and interferometry, and combine these with single particle spectra to derive phase space densities. The phase space densities depend on temperature, chemical potentials, and velocity fields in the system. This description of the final hadronic state serves as a boundary condition for models of possible quark gluon plasma production. We vary the total size of the system by studying $PbPb$, SPb , SS and pPb collisions. We also compare our results to lower energy AGS data where the π/p ratio is much lower. This comparison shows that the freeze-out of pions and protons is coupled.

NA44 is a focusing spectrometer that uses conventional dipole magnets and superconducting quadrupoles to analyze the momentum of the produced particles and create a magnified image of the target in the spectrometer [4, 5, 6, 7, 8, 9, 10]. The systematic errors on the deuteron yields range from 14% for SPb to 9% for $PbPb$. The p and \bar{p} spectra are corrected for feed-down from Λ and Σ decays using a GEANT simulation with the (Λ/p) and (Σ/p) ratios taken from the RQMD model [9, 10, 11]. The systematic error was estimated by varying these ratios by $\pm 25\%$. These errors are slightly correlated for p and \bar{p} . Fig. 1 shows NA44 deuteron spectra and previously published proton spectra at $y = 1.9-2.3$ as a function of m_T/A [12]. The centrality is $\approx 10\%$ for SS , SPb and $PbPb$. The spectra get flatter for the larger systems consistent with a higher temperature and/or stronger sideways flow. As expected from coalescence, the slopes are similar for protons

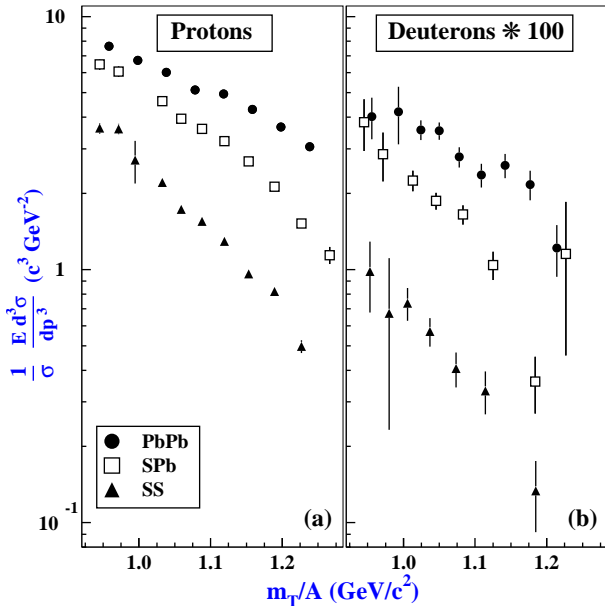


Figure 1: Invariant cross-sections vs. m_T/A at $y=1.9-2.3$, for protons (a) and deuterons (b) from central SS, SPb and $PbPb$ collisions [9, 12]

and deuterons. This was also found for lower energy data, [13]. The deuteron inverse slopes (in m_T) and yields are listed in Table 1. A comprehensive analysis of all NA44's proton and light clusters spectra will be given in a later paper.

The model of deuteron production by final state coalescence of protons and neutrons with small relative momenta states that the production of deuterons with a certain velocity is proportional to the number of protons and neutrons that have similar velocities [15, 16]. This model successfully describes measured deuteron distributions in intermediate energy heavy ion collisions and high energy pA collisions, [17]. Near mid-rapidity, direct production of $d\bar{d}$ pairs is small due to the high $d\bar{d}$ mass threshold of $3.75 \text{ GeV}/c^2$, and pre-existing deuterons are unlikely to survive the many collisions required to shift them to mid-rapidity. Since coalescence depends on the distribution of nucleons, one can determine a nucleon

System	Fit Range of $m_T - m$ MeV/c^2	Inverse Slope MeV/c^2	dN/dy (10^{-2})
SS	0-520	320 ± 149	39 ± 13
SPb	0-520	300 ± 91	153 ± 23
PbPb	160-520	379 ± 13	390 ± 20

Table 1: Deuteron inverse slopes and yields. Systematic and statistical errors have been added in quadrature. The errors are dominated by statistics and the extrapolation out of the acceptance. The PbPb fit is from [14].

source size from the ratio

$$B_2(p) \equiv \frac{\frac{E_p d^3 N_p}{dp^3} \frac{E_n d^3 N_n}{dp^3}}{\frac{E_d d^3 N_d}{dP^3}} \quad (1)$$

where the deuteron momentum P is twice the proton momentum p [18]. Since we do not measure neutrons we assume that the spectra have the same shape and take the n/p ratio to be $1.06 \pm .04$ from RQMD [11]. At $\sqrt{s_{nn}} = 4.9 \text{ GeV}$ the measured n/p ratio is $1.19 \pm .08$ independent of m_T [19]. RQMD is in reasonable agreement with this result.

To facilitate comparison with NA44's pion interferometry results, we assume a Gaussian distribution of the proton source. If one also assumes a Gaussian wave-function one can solve for the source size analytically [20]

$$(R_G^2 + \frac{\delta^2}{2})^{3/2} = \frac{3\pi^{3/2}(\hbar c)^3}{2m_p B_2} \quad (2)$$

where m_p is the proton mass and $\delta = 2.8 \text{ fm}$ accounts for the size of the deuteron. In reality the deuteron wave function is not Gaussian but is more accurately represented by the Hulthen form

$$\phi(r) = \sqrt{\frac{\alpha\beta(\alpha + \beta)}{2\pi(\alpha - \beta)}} \cdot \frac{e^{-\alpha r} - e^{-\beta r}}{r} \quad (3)$$

with $\alpha = 0.23 \text{ fm}^{-1}$ and $\beta = 1.61 \text{ fm}^{-1}$ [21]. The convolution of such a wave function with a gaussian source cannot be done analytically but is straightforward numerically to solve for the source radius R_H ,

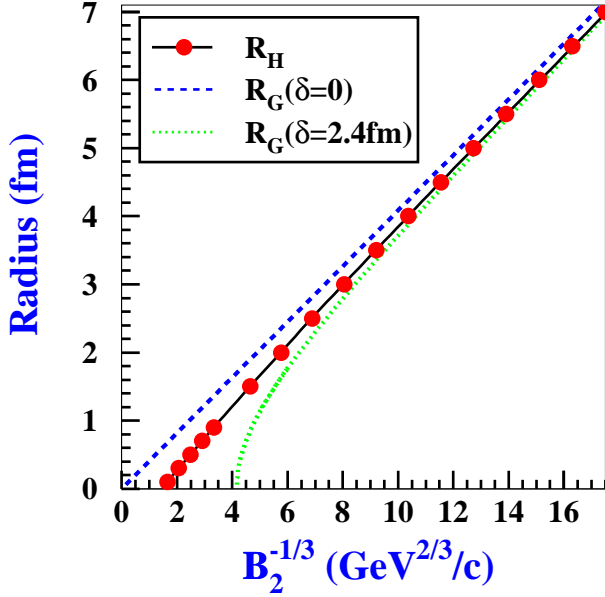


Figure 2: Comparison of proton source radii versus the coalescence parameter $B_2^{-1/3}$. R_H , shown by \bullet , is derived numerically using the Hulthen wave function in Eqn.3. The solid line is a fit to the numerical results. The dotted and dashed curves show R_G from Eqn.2 with and without a correction for the deuteron size.

[22]. Note our R_H is the R_0 of [22]. Figure 2 shows a comparison of R_H and R_G versus the coalescence parameter B_2 .

Since R_H is sensitive to both the transverse and longitudinal size of the source, when comparing to HBT results it is best to compare to $(R_\perp^2 \cdot R_\parallel)^{1/3}$ (Eqn. 6.3 of [23]), where R_\perp and R_\parallel parametrize the extent of the source perpendicular and parallel to the beam [24]. NA44 has published HBT results in the Pratt-Bertsch frame in which the sum of the longitudinal momentum of each pion pair is zero. In this scheme the radius in the sideways direction $R_s = R_\perp$ and the longitudinal radius $R_l \approx R_\parallel$ [25]. In this paper we will therefore compare R_H to $(R_s^2 \cdot R_l)^{1/3}$. These parameters can be thought of as “lengths of homogeneity” of the source [26, 27]. One can think of the radii as lengths scales of the velocity and/or tem-

perature gradients. They represent snapshots of the hadronic system at freeze-out which may occur at different times for π^+ and protons. However since the cross sections for $\pi\pi$, $p\pi$ and pp collisions are comparable the freeze-out times should be close.

A particle’s phase space density is defined as

$$f(\mathbf{p}, \mathbf{x}) \equiv (2\pi\hbar c)^3 \frac{d^6 N}{dp^3 dx^3}. \quad (4)$$

For a system in chemical equilibrium at a temperature T and chemical potential μ

$$f(E) = \frac{1}{e^{(E-\mu)/T} \pm 1} \quad (5)$$

where E is the energy and ± 1 selects bosons or fermions. For a dilute system, *i.e.* $f \ll 1$, Eqn. 5 gives

$$f_d \approx e^{-(E_d - mu_p - \mu_n)/T}. \quad (6)$$

Since $E_d = E_n + E_p$, Eqn. 6 implies that

$$f_d(\mathbf{P}, \mathbf{x}) = f_p(\mathbf{p}, \mathbf{x})f_n(\mathbf{p}, \mathbf{x}) = \frac{n}{p} \cdot f_p(\mathbf{p}, \mathbf{x})^2 \quad (7)$$

A more general form of this relation was derived in Eqn. 3 of [28] assuming only that the system is hot and large compared to the deuteron. Averaging f_p over \mathbf{x} gives

$$\langle f_p \rangle = \frac{1}{3} \frac{E_d \frac{d^3 N_d}{dP^3}}{E_p \frac{d^3 N_p}{dp^3}} \cdot \frac{p}{n} \quad (8)$$

where the factor of 3 accounts for the spin of the particles. For pions NA44 has measured the source size in 3 dimensions with HBT, as well as single particle spectra. Some of the pions come from the decay of long-lived resonances such as η , η' and ω . These pions reduce the strength of the correlation function λ , which typically is < 1 . The fraction of pions which do not come from resonances is $\sqrt{\lambda}$, [29]. This has been shown experimentally for e^+e^- collisions and for RQMD simulations of $PbPb$ collisions [30, 31]. Dividing $\sqrt{\lambda} d^3 N_\pi / dp^3$ by the Lorentz invariant volume, [27, 32, 33] gives

$$\langle f_\pi \rangle = \frac{\pi^{3/2} (\hbar c)^3}{3} \sqrt{\lambda} \frac{d^3 N_\pi}{dp^3} \frac{1}{R_s \sqrt{R_o^2 R_{long}^2 - R_{ol}^4}}. \quad (9)$$

Again the factor of 3 accounts for the pion’s spin degeneracy. Here R_l is the extent of the source along the beam direction; R_o the extent in the outward direction, ie towards the observer and R_s measures the source in the sideways direction, perpendicular to both the beam axis and the line of sight to the observer. The R_{ol} term is the “out-longitudinal” cross term [25]. For $PbPb$ collisions setting $R_{ol} = 0$ in the HBT fit increases $\langle f_\pi \rangle$ by $9\% \pm 10\%$, [6]. For pPb , SS and SPb we assume $R_{ol} = 0$ but add a systematic error of 13% to $\langle f_\pi \rangle$. For pPb deuteron spectra are not available and $\langle f_p \rangle$ was calculated using Eqn. 9, replacing the last term with $\frac{1}{R_{inv}^3}$. R_{inv} was determined from pp HBT data [7]. For $PbPb$ R_H and R_{inv} agree within their errors of $\approx 5\%$, [34].

We can test the usefulness of these coalescence methods using RQMD, coupled with a coalescence afterburner, [35]. Figure 3 shows a comparison of $\langle f_p \rangle$ and R_H for both data and RQMD for SS and $PbPb$. For the data both $\langle f_p \rangle$ and R_H are larger in $PbPb$ but for RQMD only R_H increases from SS and $PbPb$ while $\langle f_p \rangle$ stays constant. This invariance of $\langle f_p \rangle$ may be an artifact of the coalescence mechanism used, which ignores the requirement of a third particle. Since $\langle f_p \rangle$ is constant in the model the increase in proton multiplicity from SS to $PbPb$ is accommodated by a large increase in R_H . However, R_H is less than the average transverse radius of freezeout, 5.4 fm for SS and 10.3 fm for $PbPb$, indicating that coalescence is not sensitive to the full size of the source. A similar situation occurs in pion interferometry where correlations between position and momentum cause the observer to only “see” the side of the source closest to her, [6]. Since these correlations get stronger as the particles get faster the size of the source drops with m_T , [29, 36].

Figure 4 shows the system dependence of the phase space densities and source radii for π^\pm , p and \bar{p} . The p and \bar{p} radii for $PbPb$ are consistent with coalescence data at $p_T = 0$, and pp interferometry results [37, 38]. The π^+ and p phase space densities generally increase with system size. We find that

$$\langle f_{\bar{p}} \rangle \ll \langle f_p \rangle \ll \langle f_{\pi^+} \rangle < \langle f_{\pi^-} \rangle \ll 1$$

For SPb and $PbPb$ $\langle f_{\pi^+} \rangle$ was calculated in [39] using

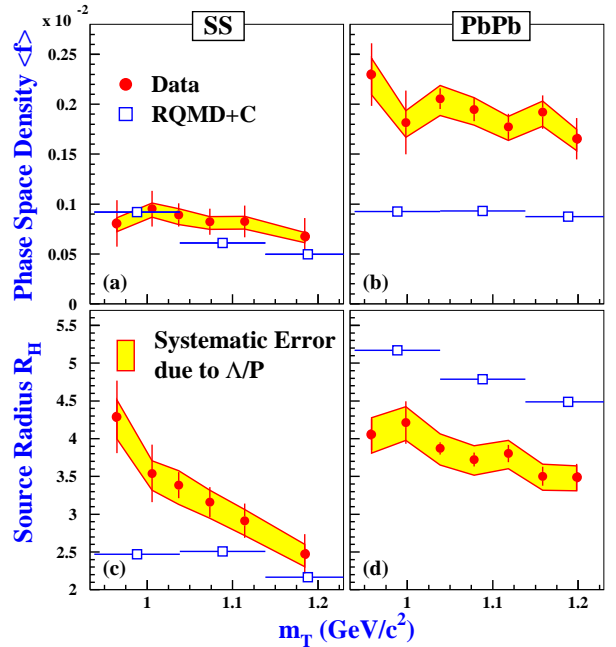


Figure 3: Proton phase space densities $\langle f_p \rangle$ (a),(b) and radii R_H (c),(d) versus m_T for $\sqrt{s_{nn}} = 17.3$ GeV for data \bullet and RQMD \square . The shaded bands indicate the estimated systematic error on the correction for weak decays.

a similar equation to Eqn. 9. However a parametrization of the pion spectrum was used rather than the spectrum itself. The authors of [39] concluded that the pion phase density was universal at freeze-out but this is not the case, since $\langle f_{\pi^+} \rangle$ is considerably smaller for pPb and SS than for SPb and $PbPb$.

For pions $(R_s^2 \cdot R_l)^{\frac{1}{3}}$ increases steadily with the number of participants and for $PbPb$ there is a rapid increase in the radii parameters with multiplicity, [8]. At low p_T R_H does not change much from SS to $PbPb$ (nor with centrality for $PbPb$) despite the increase in the proton multiplicity by ≈ 3 , see Fig. 1(a). However the m_T dependence of R_H is weaker for $PbPb$ than for SS , see Fig 3. The extra protons mainly increase the proton phase space density $\langle f_p \rangle$.

Because of their large annihilation cross-section, one might expect that antiprotons (particularly those at low p_T) would be emitted only from the surface of the system and would have a larger RMS freeze-out radius than protons. Our data are consistent with this idea. An alternative view assumes that proton and antiprotons are produced in the same volume but that antiprotons are suppressed in the interior of the source [40]. Applying this idea to our data would imply that antiprotons are emitted only from within 1.0 ± 0.2 fm of the surface [40]. Recent $AuPt$ and $AuPb$ results from E864 at $\sqrt{s_{nn}} = 4.9$ GeV and low p_T imply that $R_H^p = (4.0 \pm 0.2)$ fm, $R_H^{\bar{p}} = (2.2 \pm 0.9 \pm 0.6)$ fm and $\langle f_{\bar{p}} \rangle = (4.0 \pm 1.9) \cdot 10^{-6}$ [41]. At $\sqrt{s_{nn}} = 4.9$ GeV antiprotons are mainly produced in primary nucleon-nucleon collisions and so they may have a smaller source size than protons. Since R_H is a gaussian radius it is necessary to multiply it by $\sqrt{5}$ in order to compare it to a hard sphere with the same RMS radius, [42]. If this is done the antiproton source is roughly equal to the size of the colliding Au nuclei at $\sqrt{s_{nn}} = 4.9$ GeV.

In order to study the energy dependence of freeze-out we compare our $PbPb$ data at $\sqrt{s_{nn}} = 17.3$ GeV to AGS $AuAu$ data at $\sqrt{s_{nn}} = 4.9$ GeV. Since our data are not at mid-rapidity but at $y=2$ we have compared results at the same scaled rapidity $y = \frac{1}{3}y_{beam}$. Figure 5 shows the phase space densities and source radii for $PbPb$ and $AuAu$ collisions as a function of m_T . At a given m_T , $\langle f_{\pi^+} \rangle$ increases with $\sqrt{s_{nn}}$ while

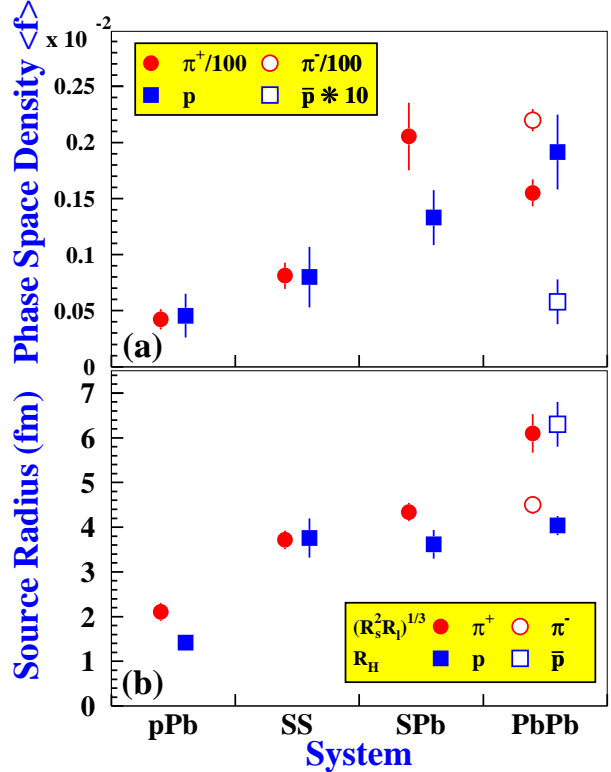


Figure 4: Phase space densities $\langle f \rangle$ and source radii for π^+ and p at $\langle p_T \rangle \approx 240$ MeV/c, and for \bar{p} at $\langle p_T \rangle \approx 490$ MeV/c. For pPb , $\sqrt{s_{nn}} = 30$ GeV and the proton points are derived from pp HBT data [7].

$\langle f_p \rangle$ decreases. Fitting $\langle f_{\pi^+} \rangle$ to Eqn. 5 gives $\mu_{\pi^+} = 0$, within errors, for both energies while μ_p/T decreases with $\sqrt{s_{nn}}$. Since $E = m_T \cosh(y)$, Eqn. 5 also implies that f be exponential in m_T for $f \ll 1$. However if the system is boosted due to transverse flow, $f(m_T)$ will become flatter [43]. This effect is proportional to mass. The data support this scenario since the $\langle f_p \rangle$ distributions are much flatter than the $\langle f_{\pi^+} \rangle$ ones. The m_T distribution of $\langle f_p \rangle$ becomes flatter as $\sqrt{s_{nn}}$ increases because of an increase in flow and/or freeze-out temperature. However in general the velocity profile cannot be determined without knowing the density profile and so a determination of a mean velocity from $\langle f_p \rangle$ is beyond the scope of this work,

[28].

Several hydrodynamical models have interpreted the HBT source radii as “lengths of homogeneity” which should decrease with increasing m_T and this is consistent with our data [26, 27]. Both pion and proton radii increase with $\sqrt{s_{nn}}$. However $\langle f_{\pi^+} \rangle$ increases with $\sqrt{s_{nn}}$ while $\langle f_p \rangle$ drops. Since $\bar{p}/p \ll 1$ at both SPS and AGS energies [9, 46, 47], we know that most protons observed near mid-rapidity are remnants of the target or projectile that were slowed down by multiple collisions. At the higher energy the protons occupy a somewhat larger volume and they are spread over a larger momentum (*i.e.* y, m_T) range. Therefore $\langle f_p \rangle$ drops with $\sqrt{s_{nn}}$.

For pions the situation is different. At $\sqrt{s_{nn}} = 4.9$ GeV, they are outnumbered by protons and so their freeze-out is driven by that of the nucleons. At $\sqrt{s_{nn}} = 17.3$ GeV, they are the most numerous particle and control freeze-out. Since $\sigma_{\pi\pi} < \sigma_{p\pi}$ $\langle f_{\pi^+} \rangle$ increases with $\sqrt{s_{nn}}$. Note that the ratio $\langle f_{\pi^+} \rangle / \langle f_p \rangle$ increases by a factor of about 16 from $\sqrt{s_{nn}} = 4.9$ GeV to 17.3 GeV while the π/p ratio only increases by a factor of 7.

Using the (anti)deuteron as a measure of the nucleon-nucleon correlations we have used a coalescence formalism to make the first measurements of p and \bar{p} source radii and phase space densities as a function of m_T at $\sqrt{s_{nn}} = 17.3$ GeV. At $\sqrt{s_{nn}} = 4.9$ GeV the antiproton source is smaller than the proton source while at $\sqrt{s_{nn}} = 17.3$ GeV it appears to be larger. We have compared the proton data to our π^+ radii and phase space densities derived from HBT and single particle results as a function of system size and $\sqrt{s_{nn}}$. This comparison reveals a linkage between proton and pion freeze-out that changes as the π/p ratio increases. At $\sqrt{s_{nn}} = 4.9$ GeV the hadronic system is held together by protons while at $\sqrt{s_{nn}} = 17.3$ GeV it is held together by pions.

We thank the NA44 collaboration for permission to publish deuteron spectra and much valuable input. Thanks also to G. Bertsch, U. Heinz, S. Mrówczyński and S. Pratt for helpful discussions.

References

- [1] P. Braun-Munzinger, I. Heppe and J. Stachel, Phys. Lett. B **465** 15 (1999).
- [2] T. Alber *et al.*, Phys. Rev. Lett. **75** 3814 (1995).
- [3] A. Ukawa, Nucl. Phys. A **638** 339c (1998).
- [4] H. Beker *et al.*, Phys. Rev. Lett. **74**, 3340 (1995); K. Kaimi *et al.*, Z. Phys. C **75** 619 (1997); H. Bøggild *et al.*, Phys. Rev. C **58**, 328 (1999) nucl-ex/9808002; H. Bøggild *et al.*, Phys. Lett. B **349** 386 (1995).
- [5] I.G. Bearden *et al.*, Phys. Lett. B **471**, 6 (1999).
- [6] I.G. Bearden *et al.*, Phys. Rev. C **58**, 1656 (1998).
- [7] H. Bøggild *et al.*, Phys. Lett. B **458**, 181 (1999).
- [8] I.G. Bearden *et al.*, “Space-time evolution of the hadronic source in peripheral to central Pb+Pb collisions.” accepted by Eur. Phys. Jour. C May 2000.
- [9] I.G. Bearden *et al.*, Phys. Rev. C **57**, 837 (1998).
- [10] I.G. Bearden *et al.*, Phys. Rev. Lett. **85** 2681 (2000).
- [11] H. Sorge, Phys. Rev. C **52**, 3291 (1995).
- [12] I would like to thank my NA44 colleagues for agreeing to publication of some of our deuteron spectra before a comprehensive paper is published.
- [13] L. Ahle *et al.*, Phys. Rev. C **60** 064901 (1999).
- [14] A. Hansen *et al.*, Nucl. Phys. A. **661** 387c (1999).
- [15] S. Butler and C. Pearson, Phys. Rev. **129**, 836 (1963).
- [16] J. Kapusta, Phys. Rev. C **21**, 1301 (1980).
- [17] H. Gutbrod *et al.*, Phys. Rev. Lett. **37** 667 (1976); S. Nagamiya, M. C. Lemaire, E. Moeller, S. Schnetzer, G. Shapiro, H. Steiner, and I. Tanihata, Phys. Rev. C **24** 971 (1981); B. V. Jacak, D. Fox, and G. D. Westfall *ibid.* **31** 704 (1985); J.W. Cronin *et al.*, Phys. Rev. D **11**, 3105 (1975).

- [18] A.Z. Mekjian, Phys. Rev. C **17**, 1051 (1978)., Nucl. Phys. A **312**, 491 (1978).
- [19] T.A. Armstrong, *et al.*, Phys. Rev. C **60** 064903 (1999).
- [20] W.J. Llope *et al.*, Phys. Rev. C **52**, 2004 (1995).
- [21] P.E. Hodgson, Nuclear Reactions and Nuclear Structure p453, Clarendon Press, Oxford, (1971).
- [22] S. Mrówczyński Phys. Lett. B **277** 43 (1992).
- [23] R. Scheibl and U. Heinz, Phys. Rev. C **59**, 1585 (1999).
- [24] U. Heinz, B. Tomášik, U.A. Wiedemann, and Y.F. Wu, Phys. Lett. B **382**, 181 (1996).
- [25] S. Chapman, P. Scotto, and U. Heinz, Phys. Rev. Lett. **74** 4400 (1995) and Heavy Ion Phys. **1** 1 (1995).
- [26] T. Csörgő and B. Lörstad, Phys. Rev. C **54** 1390 (1996).
- [27] U.A. Weidemann and U. Heinz, Phys. Rep **319** 145 (1999) nucl-th/9901094.
- [28] A. Polleri, J.P. Bondorf, and I.N. Mishustin, Phys. Lett. B **419** 19 (1998).
- [29] T. Csörgő, B. Lörstad, and J. Zimányi Z. Phys. C **71** 491 (1996).
- [30] P. Avery *et al.*, Phys. Rev. D **32** 2294 (1985).
- [31] J. Sullivan, http://p25ext.lanl.gov/people/sullivan/talks/na44/hbt_coul_poster.html
- [32] G.F. Bertsch, Phys. Rev. Lett. **72** 2349 (1994).; *ibid.* **77** (1996) 789(E).
- [33] J. Barrette, *et al.*, Phys. Rev. Lett. **78**, 2916 (1997), Nucl. Phys. A **312**, 491 (1978).
- [34] M. Murray *et al.*, Nucl. Phys. A **661** 456c (1999).
- [35] H. Sorge, J.L. Nagle, and B.S. Kumar, Phys. Lett. B **355**, 27 (1995).
- [36] Y.M. Sinukov, Nucl. Phys. A **566f** 589c (1994).
- [37] G. Ambrosini *et al.*, CERN-OPEN-99-309, New J. of Phys. **1** 22 (1999).
- [38] H. Appelshäuser *et al.*, Phys. Lett. B **467**, 21 (1999) nucl-ex/9905001.
- [39] D. Ferenc, U. Heinz, B. Tomášik, U.A. Wiedemann, and J.G. Cramer, Phys. Lett. B **457**, 347 (1999) hep-ph/9902342.
- [40] S. Mrówczyński Phys. Lett. B **308** 216 (1993).
- [41] T.A. Armstrong *et al.*, Phys. Rev. Lett. **85** 2685 (2000), nucl-ex/0005001
- [42] B. V. Jacak *et al.*, Nucl. Phys. A **590** 215c (1995).
- [43] B. Tomášik, U.A. Wiedemann, and U. Heinz, nucl-th/9907096.
- [44] R. A. Solz *et al.*, Nucl. Phys. A **661** 439c (1999).
- [45] L. Ahle *et al.*, Phys. Rev. C **57**, R466 (1998).
- [46] M.J. Bennett *et al.*, Phys. Rev. C **56**, 1521, (1997).
- [47] T.A. Armstrong *et al.*, Phys. Rev. C **59**, 2699, (1999).

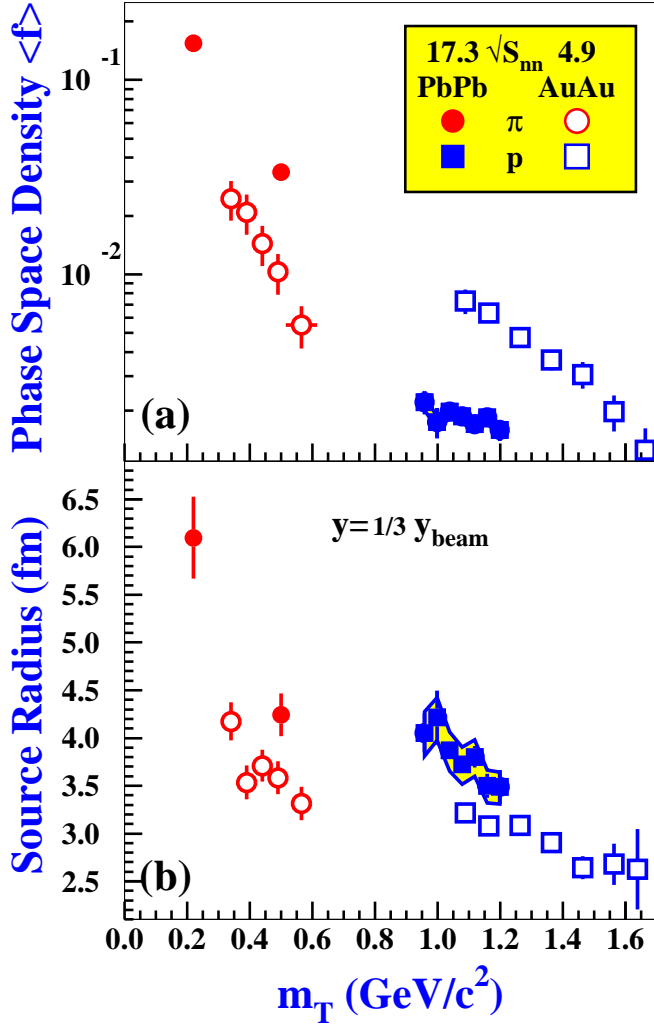


Figure 5: Phase space densities (a) and radii (b) for π^+ and p versus m_T for $\sqrt{s_{nn}} = 17.3$ and 4.9 GeV. The shaded bands indicate the estimated systematic error on the correction for weak decays. The E866 points used data from [13, 44, 45].